

Original Article

Cite this article: Cardona-Maya AM, Rojas-López JA, Germanier A, Murina P, and Venencia D. (2023) Experimental determination of breast skin dose using volumetric modulated arc therapy and field-in-field treatment techniques. *Journal of Radiotherapy in Practice*. 22(e59), 1–8. doi: [10.1017/S1460396922000292](https://doi.org/10.1017/S1460396922000292)

Received: 18 May 2022

Revised: 8 September 2022

Accepted: 16 September 2022


Key words:

breast skin dose; field-in-field; OSLD; TLD; VMAT

Author for correspondence:

José Alejandro Rojas-López, Instituto Zunino, 423 Bispo Oro, Córdoba 5000, Argentina.
E-mail: alexrojas@ciencias.unam.mx

Experimental determination of breast skin dose using volumetric modulated arc therapy and field-in-field treatment techniques

Ana María Cardona-Maya¹, José Alejandro Rojas-López^{1,2} , Alejandro Germanier³, Patricia Murina¹ and Daniel Venencia¹

¹Instituto Zunino, Córdoba, Argentina; ²Facultad de Matemática, Astronomía, Física y Computación, Universidad Nacional de Córdoba, Córdoba, Argentina and ³Unidad Estudios Físicos, CEPROCOR, Ministerio de Ciencia y Tecnología, Córdoba, Argentina

Abstract

Introduction: The use of volumetric modulated arc therapy (VMAT) on the breast has several dosimetric advantages but its impact on skin dose should be evaluated and compared to well-established treatment techniques using tangential fields. The aim of this work is to contrast the skin dose for VMAT and field-in-field (FIF) and to estimate the magnitude of the skin dose involved.

Method: The skin dose was measured, without build-up, using thermoluminescent dosimeter (TLD) and optically stimulated luminescence dosimeter (OSLD) in breast radiotherapy by an in-house anthropomorphic phantom. Two different treatment techniques were used: FIF and VMAT, based on the planning strategy proposed by Nicolini et al. The dose levels were 4300 cGy, 4600 cGy and 5600 cGy in 20 fractions. *In vivo* dosimetry with TLD for VMAT was performed for different breast sizes in the same locations as phantom measurements.

Results: The ipsilateral phantom breast skin dose using both treatment techniques was equivalent. TLD measured doses by the VMAT technique were up to 5% higher than OSLD, although they agree if we consider the geometry uncertainty of the TLD. In accordance with *in vivo* dosimetry, the mean dose of the ipsilateral breast skin was $62 \pm 6\%$ (51%, 75%) relative to the prescribed dose, regardless of the breast size for the volumes considered with this small population ($n = 9$) as shown by Mann–Whitney U-test ($Z = 1.9$, 95% confidence). The uncertainty expected in this region due to geometry (volume) changes is up to 9% higher for volumes from 225.9 cc to 968.8 cc. According to the treatment techniques and *in vivo* dosimetry, the contralateral breast skin dose was 1.0% in FIF and 2.5% in VMAT concerning the prescribed dose.

Conclusion: There is no difference in skin dosimetry between VMAT and FIF techniques on the ipsilateral breast. It provides useful support for the use of VMAT as a planning technique for breast irradiation. The work describes the importance of quantifying potential differences in skin dosimetry.

Introduction

There is evidence of skin toxicity in breast radiotherapy, especially in friction regions such as the axilla and skin folds.¹ There are multiple criteria to evaluate the degree of acute and late toxicity in the skin associated with the use of radiotherapy, such as the Radiation Therapy Oncology Group (RTOG) and the Common Terminology Criteria for Adverse Events (CTCAE). Both classifications consider acute reactions according to the severity of the injury caused to the skin. Grade 0 (G0) corresponds to unchanged skin, and late reactions after 6 months such as dermal vascularisation, skin oedema, erythema, flaky skin, fibrosis, atrophy, telangiectasia, hypo- and hyperpigmentation, necrosis and death can be found in Grades G1 to G5.^{2,3} Chronic radiation-induced skin reactions are true late-stage reactions that take months to years to develop after exposure to ionising radiation.^{3,4} Detailed context as to how breast skin dose during treatment can impact these side effects is presented in the work of Gutnik et al.⁵ Thus, there is a need to measure skin dose.

The skin dose can be defined as the deposited energy within an infinitesimally small mass of tissue on the patient's surface.⁶ The International Commission on Radiological Protection defines it as the dose at 0.07 mm depth.⁷ This magnitude can vary significantly by beam configuration parameters such as field size, surface source distance, beam modifiers (wedge), acrylic trays and oblique beam incidence.^{6,8} Furthermore, treatment modality, type of fractionation, total dose, use of bolus, concurrent chemotherapy and use of biological agents can also influence.^{1,9} For example, with respect to the use of bolus, a single institution retrospective study demonstrated a 20–30% reduction in mean skin dose when the bolus is not used in

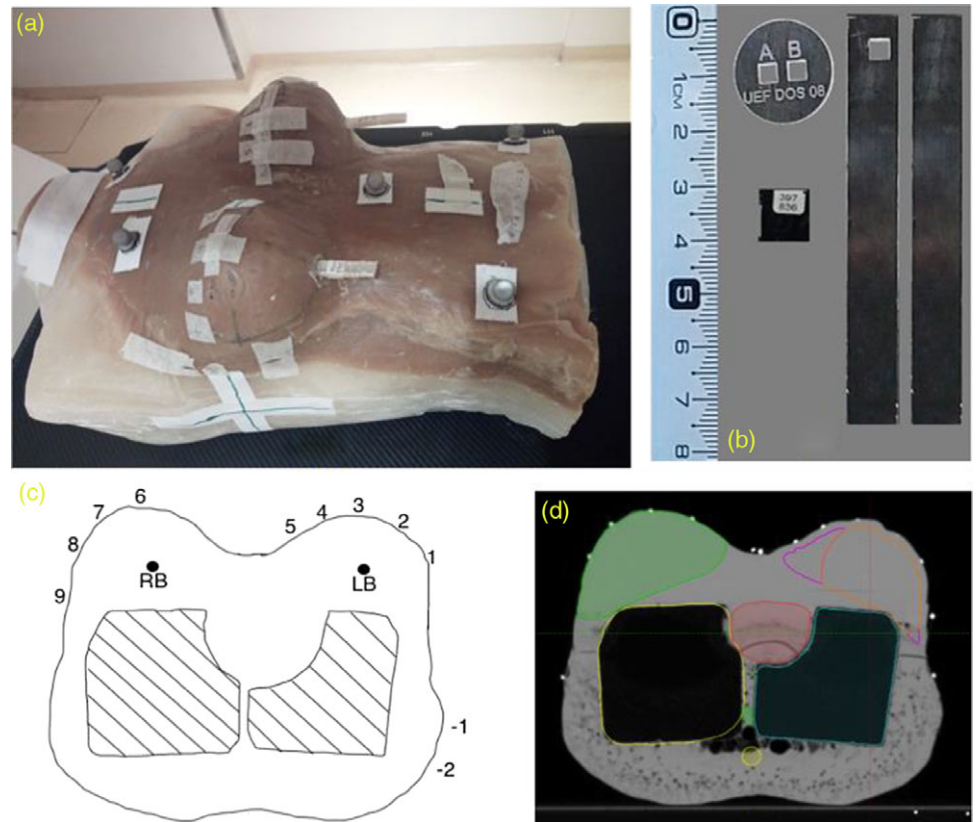


Figure 1. (a) Anthropomorphic chest phantom. (b) Polymethylmethacrylate (PMMA) devices for thermoluminescent dosimeter (TLD) and optically stimulated luminescence dosimeter (OSLD). (c) The position of each TLD/OSLD can be identified on the phantom axial view. (d) Organs at risk and planning target volumes contoured on the computed tomography.

postmastectomy radiation therapy.¹⁰ In regard to the use of chemotherapy after breast-conserving surgery, it was significantly associated with an increased incidence of G2 or greater late side effects.¹¹

The estimation of skin dose is not an easy task. Currently, treatment planning systems (TPS) can calculate the cutaneous dose (accumulation region) with an accuracy of up to 20%.¹ This is related to the dose calculation limits in areas that cover only a few millimetres in-depth and the presence of a high-dose gradient region and the lack of electronic equilibrium. The precision of skin dose assessment is essential to guarantee that the dose is below the tolerance levels and the required doses should be high enough to avoid tumour recurrence.¹

Therefore, the device used for dose measurement is important.⁶ Thermoluminescent dosimeter (TLD) and optically stimulated luminescence dosimeter (OSLD) were used in this work. The OSLD total uncertainty is 7% for the entire calibration process, taking into account heterogeneities.¹² The TLD total uncertainty is between 5 and 10%, considering the geometric factors. The choice of these detectors was based on their equivalence to tissue and their small dimensions.⁹

For many years in clinical oncology centres, the tangential field technique with multiple subfields, known as field-in-field (FIF), has been used for breast radiotherapy treatments.¹³ At present, the use of volumetric modulated arc therapy (VMAT) on the breast has been introduced, and it has turned into a more frequent technique used.^{14–16} VMAT has several dosimetric advantages but its impact on skin dose should be evaluated and compared to well-established treatment techniques using the tangential by FIF technique. The use of the VMAT technique improves the dose coverage and reduces the generation of hot spots on the field entrance. In

general, the evaluation of both techniques has focused on determining the dose coverage and homogeneity in the planning target volume (PTV) and the doses received by organs at risk (OAR).¹⁷

The objective of this work is to contrast the skin dose values for FIF and VMAT techniques and to estimate the magnitude of the skin dose involved in each therapeutic strategy. Therefore, it is proposed to evaluate the skin dose in the breast by FIF, based on the use of classical tangential beams with additional multiple static multileaf segments and weight optimisation¹⁸ and VMAT, based on the methodology proposed by Nicolini *et al.*¹⁹ By the use of TLD and OSLD on an anthropomorphic phantom, the skin dose was measured for small breast size. The phantom measurements were verified in a small sample of patients with different breast sizes (small, medium, and large). These measurements are not a patient-specific study.

Materials and Methods

Anthropomorphic phantom

An anthropomorphic chest phantom was made, as shown in Figure 1a. The phantom dimensions on the axial view were 17.5 cm x 25.3 cm, and the external–internal breast distance was 15.1 cm. For soft tissue and muscle, beeswax and paraffin were chosen, which have Hounsfield units (HU) in the range of 10 to –100. Expanded polystyrene was used for the lungs and trachea, where the HU range was –750 to –1000.

The TLDs were placed on the phantom by the use of polymethylmethacrylate (PMMA) disk-shaped devices. The OSLDs were contained in an opaque device provided by the manufacturer (Figure 1b). To place the dosimeters at a reference dose region

in charged particle equilibrium, cavities were made inside both breasts. To guarantee the correct placement of the dosimeters on the cavities (active point of measurement of the OSLD coincided with TLD), PMMA devices were made, as shown in Figure 1b.

The phantom was scanned using a Somatom Spirit unit (Siemens Healthineers, Germany). Computed tomography (CT) was done on the phantom in the supine position from the neck to the upper abdominal region. The slice thickness was 2.5 mm. The breast volume was contoured based on radiopaque flexible Teflon[®] markers. Fiducials were located along the left breast volume (PTV) and the contralateral breast where luminescent detectors were placed. Radiopaque spheres were placed for the use of positioning images with the ExacTrac[®] version 6.0 system (Brainlab AG, Munchen, Germany). The detector skin locations were placed as shown in Figure 1c at three different phantom surface regions: A, ipsilateral posterior chest wall, corresponding to points -1, -2. B, ipsilateral breast, corresponding to points 1 to 5. C, contralateral breast, corresponding to points 6 to 9.

Treatment protocol

The breast treatment planning protocol (without lymph node regions) used for this research was the one used in our institution. The dose prescription in 20 fractions for GTV-SIB (Gross Target Volume-Simultaneous Integrated Boost) was 5600 cGy, proximal CTV was 4600 cGy, and distal CTV was 4300 cGy. This gradual dose decrease concept from the tumour bed to the peripheral breast was introduced by Zunino et al.¹⁸ It was based on the hypothesis that a modest dose reduction, out of the tumour bed, would diminish normal tissue complications, including overall cosmesis, breast fibrosis, breast induration and telangiectasia.²⁰

The CT images were exported to TPS for contouring. The clinical target volume (CTV) was defined following the limits of the ring radiopaque marker placed clinically by the radiation oncologist in CT simulation. Breast CTV was divided into 3 sub-volumes: GTV-SIB, proximal CTV and distal CTV, according to Zunino et al.¹⁸ The OARs contoured were specified in Table 1. Our institution focused on the protection of the left cardiac region instead of the heart because it has a direct clinical effect on cardiovascular diseases due to relevant cardiac toxicities.^{21–23} The radiation-induced cardiovascular disease encompasses direct damage to the coronary arteries, fibrosis of the pericardium and myocardium, microvascular damage and valvular stenosis.^{24–26}

The PTVs were identified according to the nomenclature described by AAPM report TG-263.²⁷ The union of the different PTVs was created and named as zPTV_Total! The PTVs were cropped 4 mm inside the body for target evaluation in FIF. The PTVs were described by Nicolini et al. for target evaluation in VMAT. The selection of the strategy proposed by Nicolini et al. can represent a robust approach to account for moderate changes in target or body volume during the course of breast radiotherapy and to account for residual intrafractional respiratory motion in VMAT.¹⁹

Treatment unit and planning system

A Novalis Tx linear accelerator (Varian Medical Systems, Palo Alto, CA—Brainlab AG, Munchen, Germany) with high definition multileaf collimator and 6 MV energy was used. The Eclipse Treatment Planning System TPS (Varian Medical Systems, Palo Alto, CA) v.15.5 was used with the dose calculation algorithm (Anisotropic Analytical Algorithm) and a dose grid of 2.5 mm.

Table 1. Dose–volume constraints according to Zunino et al.¹⁶ for breast treatment planning with: A. field-in-field (FIF) technique (forward planning). B. Volumetric modulated arc therapy (VMAT) (inverse planning)

A. FIF		
Name	Dose–volume constraints	
zPTV_High_5600!	D95%	5320 cGy (95% of 5600 cGy)
	D2%	< 5990 cGy
zPTV_Mid_4600!	D95%	4370 cGy (95% of 4600 cGy)
zPTV_Low_4300!	D95%	4090 cGy (95% of 4300 cGy)
Ipsilateral_Lung	V20 Gy	< 10%
B. VMAT		
Name	Dose–volume constraints	
zPTV_High_5600!	D95%	5320 cGy (95% of 5600 cGy)
	D2%	< 5990 cGy
zPTV_Mid_4600!	D95%	4370 cGy (95% of 4600 cGy)
	D95%	4090 cGy (95% of 4300 cGy)
Ipsilateral_Lung	V10 Gy	< 50%
	V20 Gy	< 10%
Contralateral_Lung	V5 Gy	< 10%
SpinalCord	D _{max}	< 350 cGy
Heart_Left_Ventricle LCR (Heart Left Ventricle and LAD)	V10 Gy	< 8%
	D _{mean}	< 300 cGy left breast gating
	D _{mean}	< 150 cGy right breast
Contralateral_Breast	D _{max}	< 1000 cGy
	D _{mean}	< 200 cGy
Oesophagus	D _{max}	<4500 cGy

Heterogeneity correction was not applied. These parameters were used for both FIF and VMAT techniques.

FIF treatment plan

FIF is a forward plan based on achieving the homogeneous dose to the PTV. The plan was based on an adaptation of the FIF technique proposed by Kestin et al.¹³ An isotropic margin of 4 mm was used between the PTVs and the MLC to define the field shape to account for the beam penumbra. The isocenter was placed on the PTV as shown in Figure 2a. This was selected to provide more anatomical information for image-guided verification. This isocenter selection is related to a higher angular difference between the tangential fields.

All beam (and segment) weights were optimised manually to increase the homogeneity across the PTVs and their dose differentiation. The dose distribution obtained through the fields used in the FIF technique of breast treatment plan is shown in Figure 2a.

VMAT treatment plan

VMAT is an inverse plan based on achieving the homogeneous dose to the PTV. It was generated by the use of RapidArc[™] (Varian Medical Systems, Palo Alto, CA). The plans consisted of two semi-arcs (clockwise and counterclockwise) of 240° (from 300° to 180°) with complementary 20° collimator angles.

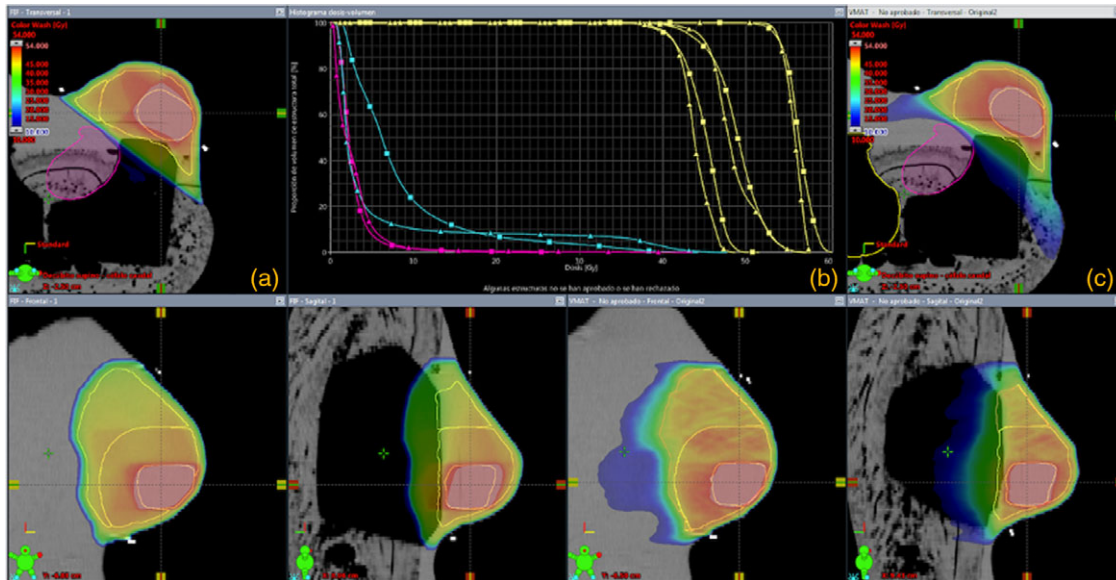


Figure 2. (a) Dose distribution for field-in-field (FIF) technique. (b) Plan comparison between FIF (triangles) and volumetric modulated arc therapy (VMAT) (squares). (c) Dose distribution for VMAT technique.

The isocenter was placed at the zPTV_Total! Center of mass. The plan was based on a reported planning strategy by Nicolini et al.¹⁹ The plan was considered acceptable if the PTV dose objectives and the constraints for the ipsilateral lung (Table 1) were achieved.

TLD dosimetry

A batch of 96 TLDs TLD-700 ($3.2 \times 3.2 \times 0.9 \text{ mm}^3$) manufactured by Bicon-NE Harshaw (USA) was used. TLDs measured dose at an equivalent tissue depth of approximately 1 mm due to their thickness and electron density.²⁷ Dosimeters were characterised and calibrated in the same treatment beam (6 MV) and read 24 hours after irradiation in the range from 10 to 280 cGy.

OSLD nanoDot dosimetry

A batch of 10 OSLD nanoDot[®] ($10 \times 10 \times 2 \text{ mm}^3$) manufactured by Landauer Inc. (Glenwood, USA) was used. The dosimeters were calibrated following AAPM TG-191 recommendations.^{28–30} Dosimeters were read on the MicroStar[®] reader (Landauer Inc, Glenwood, USA) 72 hours after exposure. Each dosimeter was read 5 times, and the average measurement (M_{raw}) was obtained.

Treatment and in vivo dosimetry

The phantom was placed on the treatment couch. Fiducials were located along the breast volume. ExacTrac[®] version 6.0 system (Brainlab AG, Munchen, Germany) was used to acquire stereotactic X-ray images to define the treatment position by fiducials. The dosimeters were placed at positions indicated in Figure 1, directly on the surface of the phantom, without bolus, in a similar way to the work of O'Grady et al.³¹ For each detector (TLD and OSLD), two different irradiations using both techniques (VMAT and FIF) were realised. The doses were compared to the prescribed dose at zPTV_High_5600!

The breast volume for the anthropomorphic phantom calculated by TPS Eclipse version 15.5 (Varian Medical Systems, Palo Alto, CA) was 306.5 cc. It corresponds to a small breast. To analyse

the skin doses reported in this work for small volumes to other breast volumes, *in vivo* measurements were performed. The size and volume of breast values were taken by the work of Zunino et al.¹⁸ The classification considered was small (160–400 cc), medium (400–700 cc) and large (700–1100 cc).

To have patient data of skin dose measurements for different breast sizes, nine patients were included in this study to have a preliminary approximation of values. The inclusion criterion was to select three patients for each breast size classification. The patients gave their informed consent. Future research on *in vivo* dosimetry will be done.

The *in vivo* dosimetry was done under the supervision of the radiation oncologist responsible for quality and protocols. The clinical control was performed by the radiation oncologist responsible once a week during the 4 weeks of the treatment. In this work, only acute (early) reactions are evaluated, given the time elapsed between the treatment irradiation and the presentation of this study. The results from the phantom study are only applicable to those with a small breast volume for patients. The complete description of the protocol, plans, TLD and OSLD dosimetry,^{28–30} manual dose calculations, *in vivo* dosimetry and patient-specific quality assurance performed by portal dosimetry^{32,33} is described in the supporting information.

Ethical considerations

The results and ethical conduct of this study have been reviewed by the Institutional Quality Committee (Comité de Calidad Institucional) from our institution. The patients gave their informed consent prior to their inclusion in the study. The *in vivo* dosimetry was done under the supervision of the radiation oncologist responsible for quality and protocols.

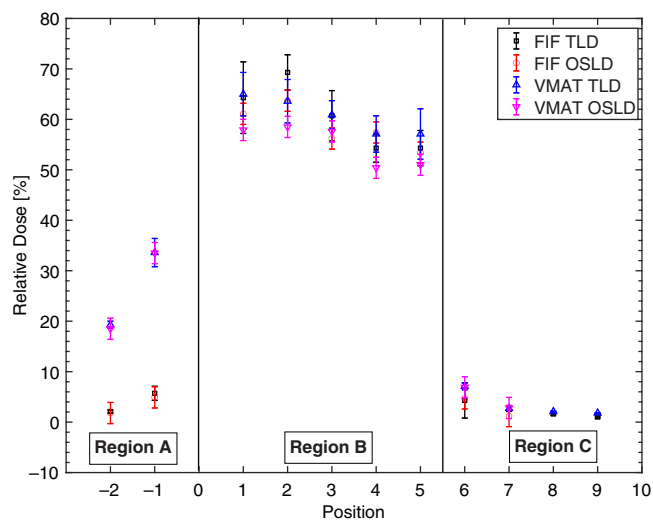
Results

Sources of uncertainties

The uncertainty of the TLD is in the range of 5 to 10%, considered as the average of two independent chips with their individual

Table 2. Physical sources of uncertainty in the skin dose measurement for thermoluminescent (TLD) and optically stimulated luminescence dosimeter (OSLD).

Procedure	Uncertainty	
Material density in phantom	10 (HU), 4% dosimetric difference	
Dosimeter calibration	5–10% for TLD	7% for OSLD
Setup	1% (1 mm)	
Total	6.5–10.8% for TLD	8.0% for OSLD

**Figure 3.** Skin dose relative to the planning target volume for the 5600 cGy dose level (zPTV_High_5600!) dose as a function of the dosimeter position. The error bars represent 1- σ SD.

sensitivity and geometrical uncertainties. Each chip has a side of 3.175 mm and is separated by 3 mm, for which the registered dose considers an area of approximately $3 \times 9 \text{ mm}^2$. The calibration dose was performed under reference conditions with the clinical beam in each batch of use of the TLD set.

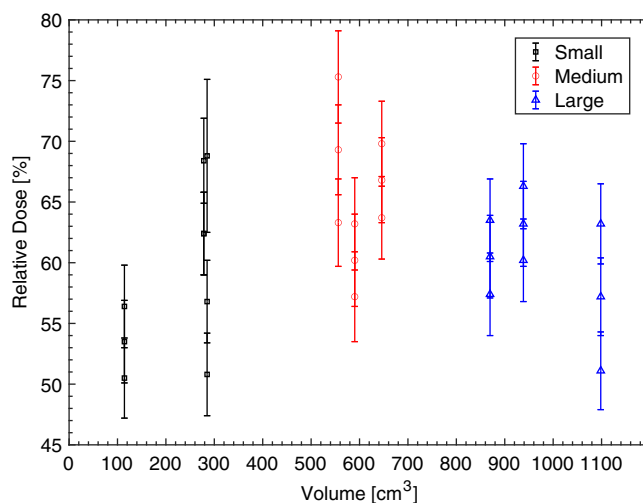
For OSLD, the system uncertainty considers the calibration process. As mentioned by Rojas-López,¹² this total uncertainty is 5%. The process takes into account the sensitivity, fading, depletion, angular factors, stability for accumulated dose, dose correction and heterogeneities interfaces. If the geometrical uncertainties (up to 5 mm) are considered, the total uncertainty is 7%.

The differences in density between the anthropomorphic phantom materials (paraffin and beeswax) and the soft tissue and muscle were studied. The differences were up to 10 HU for soft tissue (-75 HU)—beeswax (-65 HU) and up to 5 HU for (-95 HU) muscle—(-99 HU) paraffin. For VMAT treatments, the V95% 5600 cGy was 95.0% for the phantom and 96.5% for the patient cases (on average), the V95% 4600 cGy was 94.2% for the phantom and 97.6% for the patient cases (on average), and the V95% 4300 cGy was 97.0% for the phantom and 97.3% for the patient cases (on average). The HU differences implicated a dosimetric variation in a high-dose–low-gradient PTV region up to 4%.

The patients and the phantom were positioned by the use of image-guided radiotherapy (IGRT) with EPID and ExacTrac[®]; thus, the setup uncertainty was established for IGRT of 1 mm. The global uncertainty taken as the square root of the

Table 3. Skin reactions in patients treated with VMAT technique.

Skin reaction (erythema)	Patients	Onset (days)	Dose threshold (cGy)
G0	4	10	2800
G1	5	20	5600

**Figure 4.** Measurements for *in vivo* dosimetry. Relative dose as a function of breast volume for treatments performed by the volumetric modulated arc therapy (VMAT). The error bars represent 1- σ SD.

quadratic sum of all uncertainty contributions is shown in Table 2.

Anthropomorphic phantom

The skin dose is considered as the measured dose by the dosimeter at the skin surface without bolus. The relative doses to the zPTV_High_5600! for both irradiation techniques are shown in Figure 3. Relative doses were considered instead of absolute doses due to in the skin surface there is a lack of electronic equilibrium, and it cannot be assured a reliable measurement of dose. The measured dose data were converted to a relative based on the absolute mean dose to the ipsilateral breast. Measured doses are grouped into three regions for assessment. Region A corresponds to points -1 and -2 located on the left side of the irradiated breast. Region B corresponds to the points located in the ipsilateral breast, and Region C corresponds to the points located in the contralateral breast.

In particular, in zone A, corresponding to the ipsilateral posterior chest wall, the measured dose by the VMAT technique was 10% higher than the FIF technique. The difference was associated with the incidence of the beam rotation used in VMAT. This behaviour was observed using both luminescent detectors.

For region B corresponding to the ipsilateral breast, using the two-tailed Student's t-test with a 95% significance level and considering that high p -values only demonstrate that statistical significance cannot be proved, there are no statistical differences for the measured dose by both techniques ($p = 0.183$ for OSLD and $p = 0.983$ for TLD) for the phantom breast volume (small). These results show equivalence for both techniques. It was observed that the skin dose measured was from 53 to 66% and from 50 to 65% of

Table 4. Skin doses on patients for different breast volumes.

Volume (cc)	Skin dose (cGy) per fraction
Small (160–400)	164 ± 9
Medium (400–700)	182 ± 10
Large (700–110)	167 ± 10
Mean	171 ± 10

the prescribed dose to zPTV_High_5600! by the FIF and VMAT techniques, respectively. This behaviour was observed using both detectors. OSLD measured doses by the VMAT technique were up to 5% lower than TLD, although they agree if we consider the major geometry uncertainty of the TLDs due to the larger dimensions of TLD concerning OSLD and the consideration of TLD response dependency with photon field direction of incidence.³⁴

The mean skin dose measured in the anthropomorphic phantom in the region B at VMAT and FIF techniques was 59 ± 4% and 59 ± 5%, respectively, for TLD and 56 ± 3% and 58 ± 4%, respectively, for OSLD. Following the p-values, the equivalence is accepted with 5% of tolerance.

There are few studies to compare the response of different luminescent detectors. For low energies and low doses, the dosimetric measurements by OSLD showed greater sensitivity compared to the TLD dosimeters by up to 10%.^{28,33,34} The scatter radiation, the OSLD angular dependence concerning the primary radiation beam, the contribution of out-of-field doses and the lack of electronic equilibrium³⁵ at certain angles for the VMAT technique would explain the discrepancies found in experimental values.

For region C corresponding to the contralateral breast, the relative values by both techniques were from 1.0 to 2.5% concerning the prescribed dose of PTV-SIB. The two semi-arcs from 300° to 179° used by the VMAT technique explained the dose at these points. Dose reduction in the contralateral breast using VMAT can be improved by the use of avoidance sectors. It is achieved by the use of the avoidance sector on the beam's eye view arcs superposition on the contralateral breast region and the PTV or by the arcs splitting.

In vivo dosimetry

In accordance with *in vivo* dosimetry measured at the same points (with respect to the phantom) for the nine patients with different breast volumes (small, medium and large), the mean dose of the ipsilateral breast was 62 ± 6% relative to the prescribed dose to zPTV_High_5600! regardless of the breast size. The results are shown in Figure 4. This result contrasted with the known dose increment with respect to breast volume in the FIF modality.³⁶ The uncertainty expected in this region due to geometry (volume) changes is up to 9% higher for volumes from 225.9 cc to 968.8 cc.

Acute skin toxicity was evaluated in the studied patients at the mid-treatment and the end of the treatment. In the middle of the treatment, no patient presented changes on the skin. The evaluation was classified according to the criteria of the RTOG/CTCAE as G0. At the end of the treatment, four patients did not present any changes in the skin (G0). The rest of the patients had G1 skin reactions.

The mean relative dose of the irradiated breast skin was 62 ± 6% (51%, 75%) relative to the prescribed dose, regardless of the breast size for the volumes considered with this small population ($n = 9$) as shown by the Mann–Whitney U-test ($Z = 1.9$, 95% confidence).

The Mann–Whitney U-test was used as an alternative when the samples did not come from populations with a normal distribution or when the samples were too small in size. In the middle of the treatment, the accumulated dose in the skin would be approximately 1700 cGy, and at the end of the treatment, it would be 3400 cGy. Therefore, depending on these results and the reported in Table 3, the skin toxicity was independent of the breast volume.

In terms of skin dose in patients, the mean values for different breast sizes were summarised in Table 4 where the doses (measured by TLD) of the irradiated breast skin were considered. The mean breast skin dose for the patient sample was 171 ± 10 cGy per fraction.

Quality assurance and dosimetric parameters

Concerning the quality of the phantom and patient plans, the independent MU calculations performed by RadCalc v6.3 are in agreement with the confidence level of 5%. The patient-specific quality assurance by portal dosimetry by different gamma criteria is in agreement in all cases (90% tolerance) for individual arcs as shown in the supporting information for the patient and phantom plans.

The dose–volume constraints for the OARs fulfilled the institutional protocol (Table 1) according to Zunino et al.¹⁸ PTV dose conformity for the three dose levels is shown in the supporting information, considering the Paddick conformity index 5600 cGy, GI 5600 cGy, V95% and D_{mean} .

Discussion

The ipsilateral phantom breast skin dose using both treatment techniques (FIF and VMAT) was equivalent within the range from 50 to 66% of the prescribed dose to zPTV_High_5600! TLD measured doses by the VMAT technique were up to 5% higher than OSLD, although they agree if we consider the physical sources of uncertainties (as shown in Table 2) and the big geometry uncertainty of the TLD.

In addition, for *in vivo* dosimetry, the mean dose of the ipsilateral breast skin was 62% (on average) relative to the prescribed dose, regardless of the breast size. The contralateral breast skin dose (region C on the anthropomorphic phantom) was 1.0% in FIF and 2.5% in VMAT concerning the prescribed dose, regardless of the dosimeter used.

In particular, for the FIF treatment modality, the skin dose is proportionally related to the breast volume by the distance between the entrance of internal and external fields. A first approach to deal with the increment of skin dose in large breast volume in the FIF technique is to use higher energies. The inconvenience of higher energies is the subdosage on the surface at the field entrance. The use of the VMAT technique improves the dose coverage¹⁹ and reduces the generation of hot spots on the field entrance, unlike the FIF technique.

Dias et al.¹ measured cutaneous dose with and without bolus in anthropomorphic phantom and patients through Metal Oxide Semiconductor Field Effect Transistors (MOSFETs) and compared them with calculated values by the TPS in three-dimensional Conformal Radiotherapy (3DCRT) and VMAT techniques. Dias et al. reported differences between TPS and measurements within the TPS imprecision error range of ± 20% for the accumulation zone.¹ The surface dose with the presence of bolus increased in the VMAT technique. Toossi et al.³⁷ compared estimated cutaneous dose by Monte Carlo simulations with measured dose using radiochromic film on a phantom with tangential and medial fields.

Toossi et al. concluded that 18.7% of the points of interest located on the skin showed doses that could cause early and late skin reactions.³⁷ However, due to the limited information where skin dose is evaluated and compared in intensity-modulated radiotherapy techniques with FIF modality and VMAT in breast cancer, the need arises to know its impact on toxicity and breast aesthetic appearance with both techniques.

The relative doses to the zPTV_High_5600! measured in the anthropomorphic phantom showed equivalence between both techniques in the ipsilateral and contralateral breast regions. The unique difference measured was in the axillary region. It was associated with the incidence of the beam rotation used in VMAT. The PTV dose conformity in the three dose levels and the patient-specific quality assurance for phantom and patients' plans showed good results in relation to dose objectives. The FIF disadvantages are not observed in the VMAT technique due to the shape and multiple field entrances produced by arcs. The phantom skin measurements showed correspondence between both techniques in the ipsilateral breast for a small volume. This result establishes that the unique dose skin increment in the VMAT technique is in the axillary region.

The skin dose associated with the most common acute radiation reactions is described by Kole et al.³⁸ The authors showed that between the first 7 to 10 days after the start of treatment, erythema is the first clinically evident symptom. It can progress and evolve into oedema, dryness and burning, as well as changes in sensitivity and colour of the breast (hyperpigmentation). The associated dose ranges are from 600 to 2000 cGy. Dermal symptoms such as dry scaling (G1 toxicity) and wet scaling (G2 toxicity) usually appear at the end of the treatment, approximately from 3 to 4 weeks or more. They are associated with accumulated doses higher than 2000 and 3000 cGy, respectively. The symptoms such as ulceration (G3 to G4 toxicity) are related to doses greater than 4000 cGy and appear after 5 weeks or more. Prospective trials by Pignol et al. and Harsolia et al. showed better cosmetic results with a lower rate of hyperpigmentation, oedema and wet scaling^{39,40} by the shorter time of symptomatic appearance and level of radiation dermatitis reactions.³⁶

Following the VMAT treatment technique, for the nine patients, no changes on the skin were presented (G0) at the mid-treatment as shown in Table 3. The *in vivo* dosimetry performed in this study is bounded to small, medium and large breast volumes. The pendulous breasts and the inframammary fold region will be studied in future work. The inframammary fold region, which is a complex region due to its geometry, can lead to high-dose uncertainties related to angular geometry, lack of electronic equilibrium and anatomical movements.

In addition, in these published works,^{37–40} it was mentioned that radiotherapy delivered with modern techniques, such as VMAT, allows the dose homogeneity improvement in the volume breast and the reduction of the skin dose when the purpose is to irradiate the lymph nodes. Thereby, a lower rate of acute and chronic epidermal toxicity was observed. There is clinical evidence showing, for example, that telangiectasia is a late sequela of acute skin reactions and that dose inhomogeneity led to an increased risk of fibrosis and inferior cosmetic outcome.^{37–40}

Limitations

This work is circumscribed to the experimental determination of breast skin dose in FIF and VMAT techniques on the anthropomorphic phantom. *In vivo* dosimetry was evaluated for a few

patients. The detailed and conclusive clinical study of skin cutaneous reactions will be studied in future work with a large number of patients.

In this study, we evaluated the skin dose in small breast size (for anthropomorphic phantom and patients), medium and large (for patients). It is necessary to evaluate, in future work, the skin dose in pendulous breasts and in the region of the breast fold.

Conclusions

The ipsilateral breast skin dose measured in an anthropomorphic phantom by the use of luminescent dosimeters using VMAT (proposed by Nicolini et al.) and FIF is equivalent. The skin dose measured by TLD in VMAT for different breast sizes was 171 ± 10 cGy on average, and the skin reactions reported were at most G1 for 5 patients. Following the institutional dose–volume constraints reported in this study, the VMAT technique ensured better dose constraints to organs at risk compared to the FIF technique.

This work suggests the study of the skin dose in pendulous breasts and in the region of the breast fold with luminescent dosimeters.

Supplementary Material. To view supplementary material for this article, please visit <https://doi.org/10.1017/S1460396922000292>.

Acknowledgements. The authors thank Fundación Marie-Curie for the phantom financial support, M.Sc. Héctor Agüero and the health radiophysics service of the School of Nuclear Medicine Foundation (FUESMEN) for providing the OSL nanoDot batch, dosimetrists Nicolás Picatto and Franco Barolo for their support in the phantom construction, Omar Briones for reviewing the manuscript.

Funding. This research received no specific grant from any funding agency in the public, commercial or not-for-profit sectors.

Conflict of Interests. We have no conflicts of interest to disclose.

References

1. Dias A G, Pinto D F S, Borges M F et al. Optimization of skin dose using *in vivo* MOSFET dose measurements in bolus/non-bolus fraction ratio: a VMAT and a 3DCRT study. *J Appl Clin Med Phys* 2019; 20 (2): 63–70.
2. Huang C J, Hou M F, Luo K H et al. RTOG, CTCAE and WHO criteria for acute radiation dermatitis correlate with cutaneous blood flow measurements. *Breast* 2015; 24 (3): 230–236.
3. Hymes S R, Strom E A, Fife C. Radiation dermatitis: clinical presentation, pathophysiology, and treatment 2006. *J Am Acad Dermatol* 2006; 54: 28–46.
4. Wei J, Meng L, Hou X et al. Radiation-induced skin reactions: mechanism and treatment. *Cancer Manag Res* 2019; 11: 167–177.
5. Gutkin P M, Fernandez-Pol S, Horst K C. Erythema of the skin after breast radiotherapy: it is not always recurrence. *Int Wound J* 2020; 17 (4): 910–915.
6. Alashrah S, Kandaiya S, Maalej N, El-Taher A. Skin dose measurements using radiochromic films, TLDs and ionisation chamber and comparison with Monte Carlo simulation. *Radiat Prot Dosimetry* 2014; 162 (3): 338–344.
7. Kry S F, Smith S A, Weathers R, Stovall M. Skin dose during radiotherapy: a summary and general estimation technique. *J Appl Clin Med Phys* 2012; 13 (3): 20–34.
8. Kim S, Liu C R, Zhu T C, Palta J R. Photon beam skin dose analyses for different clinical setups. *Med Phys* 1998; 25 (6): 860–866.
9. Devic S, Seuntjens J, Abdel-Rahman W et al. Accurate skin dose measurements using radiochromic film in clinical applications. *Med Phys* 2006; 33 (4): 1116–1124.

10. Wong G, Lam E, Bosnic S *et al.* Quantitative effect of bolus on skin dose in postmastectomy radiation therapy. *J Med Imaging Radiat Sci* 2020; 51 (3): 462–469.
11. Toledano A, Garaud P, Serin D *et al.* Concurrent administration of adjuvant chemotherapy and radiotherapy after breast-conserving surgery enhances late toxicities: long-term results of the ARCOSEIN multicenter randomized study. *Int J Radiat Oncol Biol Phys* 2006; 65 (2): 324–332.
12. Rojas J A. Dosimetría in vivo con el Uso de OSL nanoDot en Radioterapia con Intensidad Modulada. Universidad Nacional de Cuyo, Argentina: Comisión Nacional de Energía Atómica, 2019: 12–33.
13. Kestin L L, Sharpe M B, Frazier R C *et al.* Intensity modulation to improve dose uniformity with tangential breast radiotherapy: initial clinical experience. *Int J Radiat Oncol Biol Phys* 2000; 48 (5): 1559–1568.
14. Johansen S, Cozzi L, Olsen D R. A planning comparison of dose patterns in organs at risk and predicted risk for radiation induced malignancy in the contralateral breast following radiation therapy of primary breast using conventional, IMRT and volumetric modulated arc treatment techniques. *Acta Oncol* 2009; 48 (4): 495–503.
15. Boman E, Rossi M, Haltamo M, Skyttä T, Kapanen M. A new split arc VMAT technique for lymph node positive breast cancer. *Physica Med* 2016; 32 (11): 1428–1436.
16. Bradley JA, Mendenhall N P. Novel Radiotherapy Techniques for Breast Cancer. *Ann Rev Med* 2018; 69: 30.1–30.12.
17. Unnithan J, Macklis R M. Contralateral breast cancer risk. *Int J Radiat Oncol Biol Phys* 2003; 55 (3): 239–246.
18. Zunino S. Breast sub-volumes: preliminary results of a new concept to gradually decrease the dose from the tumor bed to the peripheral breast using simplified IMRT. *Global J Breast Cancer Res* 2016; 3 (2): 27–32.
19. Giorgia N, Antonella F, Alessandro C, Eugenio V, Luca C. Planning strategies in volumetric modulated arc therapy for breast. *Med Phys* 2011; 38 (7): 4025–4031.
20. Mukesh M, Harris E, Jena R, Evans P, Coles C. Relationship between irradiated breast volume and late normal tissue complications: a systematic review. *Radiother Oncol* 2012; 104 (1): 1–10.
21. Early Breast Cancer Trialists' Collaborative Group (EBCTCG). Effects of radiotherapy and of differences in the extent of surgery for early breast cancer on local recurrence and 15-year survival: an overview of the randomised trials. *The Lancet* 2005; 366(9503): 2087–2106.
22. Cuzick J, Stewart H, Rutqvist L *et al.* Cause-specific mortality in long-term survivors of breast cancer who participated in trials of radiotherapy. *J Clin Oncol* 1994; 12: 447–453.
23. Darby S. Research pointers: mortality from cardiovascular disease more than 10 years after radiotherapy for breast cancer: nationwide cohort study of 90 000 Swedish women. *BMJ* 2003; 326 (7383): 256–257.
24. Tapio S. Pathology and biology of radiation-induced cardiac disease. *J Radiat Res* 2016; 57 (5): 439–448.
25. Adams M J, Hardenbergh P H, Constine L S, Lipshultz S E. Radiation-associated cardiovascular disease. *Crit Rev Oncol Hematol* 2003; 45 (1): 55–75.
26. Stewart F A, Seemann I, Hoving S, Russell N S. Understanding radiation-induced cardiovascular damage and strategies for intervention. *Clin Oncol* 2013; 25 (10): 617–624.
27. Mayo C S, Moran J M, Bosch W *et al.* American Association of Physicists in Medicine Task Group 263: Standardizing Nomenclatures in Radiation Oncology. *Int J Radiat Oncol Biol Phys* 2018; 100: 1057–1066.
28. Kry S F, Alvarez P, Cygler J E *et al.* AAPM TG 191: Clinical use of luminescent dosimeters: TLDs and OSLDs. *Med Phys* 2020; 47 (2): e19–e51.
29. Viamonte A, da Rosa L A R, Buckley L A, Cherpak A, Cygler J E. Radiotherapy dosimetry using a commercial OSL system. *Med Phys* 2008; 35 (4): 1261–1266.
30. International Atomic Energy Agency. Implementation of the International Code of Practice on Dosimetry in Radiotherapy (TRS 398): Review of Testing Results. Vienna: International Atomic Energy Agency, 2005: 102.
31. O'Grady F, Barsky A R, Anamalayil S *et al.* Increase in superficial dose in whole-breast irradiation with halcyon straight-through linac compared with traditional C-arm linac with flattening filter: in vivo dosimetry and planning study. *Adv Radiat Oncol* 2020; 5 (1): 120–126.
32. Esch A V, Huyskens D P, Hirschi L, Scheib S, Baltes C. Optimized varian aSi portal dosimetry: development of datasets for collective use. *J Appl Clin Med Phys* 2013; 14 (6): 82–99.
33. Rojas-López J, Venencia D. Importance of beam-matching between true-beam STx and novalis Tx in pre-treatment quality assurance using portal dosimetry. *J Med Phys* 2021; 46 (3): 211–220.
34. Rojas-López J A, López-Pineda E, Reynoso-Mejía C A, Brandan M E. Dependence of the TLD-300 glow curve on the photon field direction of incidence. Studies in air and in phantom for mammography and CT x-rays. *AIP Conference Proceedings* 2019; 2090: 030007-1–030007-7. American Institute of Physics Inc.
35. Ramos-Avasola S, Karstulovic C, Gamboa C, Gamarra J, Catalán M. Son reproducibles las mediciones dosimétricas a bajas dosis en cardiología intervencionista? *Rev Chil Radiol* 2016; 22 (2): 70–75.
36. Freedman G M, Li T, Nicolaou N, Chen Y, Ma C C M, Anderson P R. Breast intensity-modulated radiation therapy reduces time spent with acute dermatitis for women of all breast sizes during radiation. *Int J Radiat Oncol Biol Phys* 2009; 74 (3): 689–694.
37. Bahreyni Toossi M T, Mohamadian N, Mohammadi M *et al.* Assessment of skin dose in breast cancer radiotherapy: on-phantom measurement and Monte Carlo simulation. *Rep Pract Oncol Radiother* 2020; 25 (3): 456–461.
38. Kole A J, Kole L, Moran M S. Acute radiation dermatitis in breast cancer patients: challenges and solutions. *Breast Cancer* 2017; 9: 313–323.
39. Pignol J P, Olivetto I, Rakovitch E *et al.* A multicenter randomized trial of breast intensity-modulated radiation therapy to reduce acute radiation dermatitis. *J Clin Oncol* 2008; 26 (13): 2085–2092.
40. Harsolia A, Kestin L, Grills I *et al.* Intensity-modulated radiotherapy results in significant decrease in clinical toxicities compared with conventional wedge-based breast radiotherapy. *Int J Radiat Oncol Biol Phys* 2007; 68 (5): 1375–1380.